A proof of concept study for a fast acquisition in a LEO satellite GPS receiver

C. ALCAIDE-GUILLÉN and A. VIDAL-PANTALEONI, Universitat Politècnica de València, Spain.

J.R. MARTÍN- ROMERO, Instituto Nacional de Técnica Aeroespacial, Spain.

ABSTRACT: *The aim of this work is to perform a proof of concept study in order to assess if the pre-correlation differential detector can be used to tackle the GPS signal acquisition in a high dynamics scenario problem. The high dynamics scenario to be studied is the case in which a GPS receiver is used in a LEO (Low Earth Orbit) satellite mission. The receiver's appropriateness for the case study is demonstrated via computational cost study and detector statistical characterization. GPS L1 C/A legacy signals for the context are simulated using a Spirent GSS7700 signal generator. The signals are sampled using a USRPX310 as a RF front-end. Using these samples, the receivers are implemented in Matlab using a SDR (Software Defined Radio) experimental setup. A specially designed figure of merit is used to measure the performance of the pre-correlation differential receiver in the realistic LEO satellite case study.*

INTRODUCTION

The purpose of a GNSS receiver signal-processing chain is to obtain the necessary information for positioning. To accomplish this goal, the receiver must be able to detect if the signal is present and must provide a first coarse estimate of the signal code phase and Doppler frequency. This first step in the GNSS signal processing sequence is known as signal acquisition. In order to estimate the two parameters, the receiver needs to explore different possible combinations of code phase and Doppler frequency. In this work, a specific receiver acquisition solution for LEO embedded GPS receivers is studied.

The requirements for a LEO embedded GNSS receiver are different from the requirements for a ground application, due to the fast LEO satellite movement and to the different environmental conditions. The requirements for a LEO GNSS application are described below.

1. In many LEO scenarios, the signal level is higher than the nominal signal level [1-3]. Moreover, signal distance travel is reduced, no tropospheric effects are present and ionospheric effect is typically smaller [4] (except for low elevation satellites). In this scenario there is no need to use sensitivity enhancing algorithms [5-9], so it is interesting to test methods that work well only for high signal levels.
2. For LEO scenarios, the Doppler search span value is 100 kHz, instead of 10 kHz, which is the typical search span value for a static user [10]. The increased Doppler search translates into a bigger computational cost. Code Doppler takes values in the interval that spans from 50 Hz/s to 75 Hz/s [1],[3]. These features represent the two main challenges in the LEO scenario.
3. In many LEO satellites power is limited, and the receiver is turned on and off in many occasions [2], therefore it is necessary to consider using computationally efficient algorithms.
4. For LEO scenarios, the satellite passes can vary from 20 to 50 minutes [1], therefore it is necessary to perform a fast acquisition.

In light of the points presented, when designing a GPS receiver for LEO space applications, the Doppler frequency search space must be adapted to be able to detect the satellite signal. The code Doppler effect must be taken into consideration too.

In other studies, dealing with LEO GNSS receivers such as [11], a standard non-coherent acquisition method is successfully used to tackle the problem. In [1] a computationally efficient method based on [9] is applied for the case for GPS and GALILEO signals. The two approaches successfully deal with solving the problem, but they still perform the computationally costly Doppler frequency search.

In this work, we propose the usage of the pre-correlation differential detector. This detector type need not perform a Doppler search, [5-6], and this is why this detector is considered to perform the best in terms of sensitivity to dynamics. In [12], it is stated that the major drawback in the usage of this detector, is the fact that a longer integration time (in comparison to other detectors), is required to acquire signals. Nevertheless, in a LEO scenario, the signal level is generally high and it is appealing to take advantage of the higher acquisition threshold.

A proof of concept study to find out if the pre-correlation differential detector performs as expected in a realistic simulation environment is performed. The receiver sensitivity to input Doppler frequency and data modulation is measured and hence the performance of the pre-correlation differential receiver/detector is assessed. Some different implementations of the detector are studied to investigate if these forms help in improving the performance of the baseline pre-correlation differential detector. These detectors are characterized in statistical fashion. The distinct implementations will differ in the way in which the decision statistic is formed. The performance is measured by means of an ad-hoc figure of merit. The speed-up achieved using the pre-correlation differential detector, instead of the standard baseline non-coherent receiver is quantified. Moreover, a method which is not computationally burdensome is tested to provide an estimate for the Doppler frequency.

THEORETICAL ASPECTS

Doppler frequency study

The Doppler dilation or contraction, arising from the relative motion between the GPS satellite and the receiver, which manifests as a time-varying carrier and code Doppler shift, must be considered when designing GPS detectors. To give some context on the realistic case study, some calculations to determine the theoretical maximum Doppler frequency shift are performed.

The L1 frequency value in the case Doppler effect exists is named $f_{L1}{}'$, and can be expressed in the following form, [10] and [13].

$$f_{L1}{}' = \left(\frac{c+V_L}{c-V_S}\right) \cdot f_{L1} \quad (1)$$

c: Stands for the speed of light in free space.
$f_{L1}{}'$: Doppler shifted L1 frequency.
f_{L1}: L1 frequency.
V_L: LEO satellite velocity component.
V_L: GPS satellite velocity component.

For a 1000 km LEO, the values for V_L and V_s that maximize equation (1) are approximately 7.060 km/s and 1.014 km/s, respectively. If we define the Doppler frequency deviation f_d, as the difference between the nominal L1 frequency and the actual frequency received, then it follows that:

$$f_d = f_{L1}{}' - f_{L1}. \quad (2)$$

The substitution of these values into equation (1), yields the following result.

$$f_{L1}{}' = 1.57542 \cdot 10^9 \cdot \left(\frac{3\cdot10^8+7.060\cdot10^3}{3\cdot10^8-1.014\cdot10^3}\right) = 1.575462 \cdot 10^9 \quad (3)$$

Therefore

$$f_d = f_{L1}{}' - f_{L1} = 42.4\ kHz \quad (4)$$

The ratio between the nominal L1 frequency and the C/A code chip frequency is 1540, so the Doppler shift translates into a code Doppler shift of $\frac{f_d}{1540}$ Hz. Therefore, every chip drifts:

$$\frac{f_d}{1540\cdot1.023\cdot10^6} \text{ chips} \quad (5)$$

Hence in 1 ms the code will drift

$$\frac{f_d\cdot1023}{1540\cdot1.023\cdot10^6} \text{ chips.} \quad (6)$$

If $f_d = 42.4\ kHz$, in 1 ms, the code drifts 0.0275 chips. For a 0.5 chip drift to occur, a $\frac{f_d}{1540}$= 18.16 ms integration time must be used. It is worth mentioning that code Doppler effect is much more harmful for wider band GNSS signals than for the C/A L1 signal.

For a 200 km LEO orbit the f_d value is 45 kHz, so accounting for the worst-case LEO scenario, the Doppler search space spans from -45 kHz to 45 kHz. In [1], a search space from -42 kHz to 42 kHz is used for a 300-km altitude LEO case study.

At this point, it is wise to widen the frequency search space to gain some margin by adding 5 kHz to the search space, especially considering the receiver's clock drift must be considered too. Taking these points into consideration, the span of the search space for the LEO GNSS receiver is 100 kHz.

When working with the GPS L1 C/A legacy signal, it is necessary to explore the 1023 possible code phase values. The width of the Doppler frequency search range depends on the relative velocity between the GPS satellite and the receiver. According to [10] and [14-15], the search space width for an earth-based receiver must be 10 kHz, accounting for a search range starting at -5 kHz and ending at 5 kHz. Considering the search space width is multiplied by a factor of ten, when comparing the earth-based static receiver with the LEO orbit satellite embedded receiver, it is appealing to study a method, which need not search in the two search dimensions.

Baseband signal model

To fully understand the effects of a GNSS signal in a high dynamic platform, a baseband signal model (the signal is downconverted and the f_{L1} frequency is eliminated) is presented. This model is only valid for small integration times, as it is assumed that the Doppler carrier and code, are constant when the integration time is small. The signal model is the one used in [5]. The model only considers the signal transmitted by one satellite, because it is a suitable

assumption for this study. The near-far effect will not be studied in this work.

The signal model used is presented below.

$$\varepsilon = \sqrt{P(nT_s)} \quad (7)$$

$$S = \varepsilon \cdot D(nT_s) \cdot C\left(nT_s - \varsigma T_{chip}\right) \cdot e^{jw_d nT_s + \theta_k} + n_w(nT_s) \quad (8)$$

T_s: Sampling period.
n: Number of signal sample.
D: Data signal.
P: Signal power.
C: GPS L1 C/A Gold code.
T_{chip}: Chip period.
w_d: Signal Doppler angular frequency.
θ_k: Signal carrier random phase.
ς: Code phase offset.
$n_w(nT_s)$: Function modeling the channel's additive Gaussian noise.

According to [5] and [11], $n_w(nT_s)$ can be described using a complex normal distribution, composed of a real and an imaginary part, which are jointly normal and independent.

The receiver evaluates how well each of the possible frequency-phase combinations estimate the GNSS signal parameters. In this way, a two-dimensional search space is formed. The pre-correlation differential detector only needs to search the code phase space, so just a one-dimensional search space must be explored instead of a two-dimensional search.
The parameters involved in the 2-D search space are the following:

ς: Code phase offset, which is one of the parameters in the search space.
f_d: Doppler frequency, which is one of the parameters in the search space.
$\Delta\varsigma$: Code search spacing, i.e. the step used in exploring the code phase search space.
Δf_d: Doppler frequency search spacing, i.e. the step used in exploring the Doppler frequency search space.

The interest in studying the pre-correlation differential detector arises from the fact this type of detector need not explore the frequency search space to detect the presence of a GNSS signal. This fact is particularly interesting in a situation in which the Doppler search space is wide. In these wide Doppler search space scenarios, the use of this type of receivers is interesting because a great reduction in the computational burden associated to the acquisition process can be achieved.

Residual effects are a key aspect affecting receiver performance. The focus is set in quantifying how much these factors affect the receiver performance in this case.

The effect of the following factors is studied:

- Doppler carrier frequency.
- Residual phase offset.
- Data modulation.

A statistical analysis is performed to compare groups of signals with different Doppler frequencies, and groups whose signals are modulated or unmodulated by GPS data navigation information. By studying the aspects affecting the receiver performance, the receiver usage suitability for the case study can be assessed.

Receiver working principle and general aspects

The block diagram of the pre-correlation detector is presented in Figure 1. This receiver appears as the pre-correlation differential detector in [6], as the differentially coherent detector in [5] or as the pre-detector differential scheme in [1] and [16]. The 'delay and multiply method' in [10] and [17] applies the same concept but works with an IF (Intermediate Frequency) signal, instead of a baseband signal.

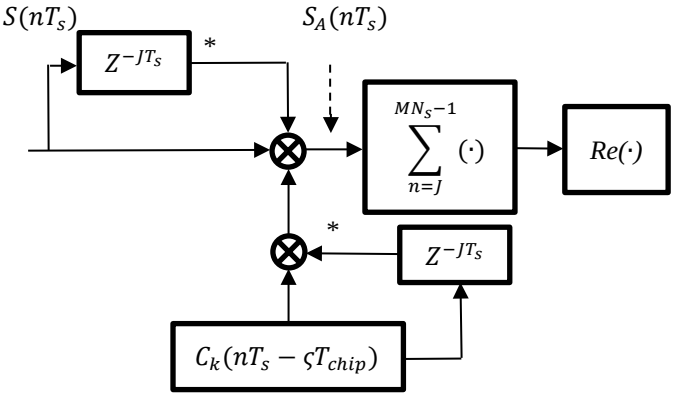

Fig. 1- Pre-correlation differential detector. (Type 1 detector).

The symbol *, stands for complex conjugation. The input signal is delayed an integer number of samples (J), and correlated with a Gold code generated as the product of two Gold codes. Finally, the decision statistic is formed by taking the real part of the correlation. N_s is the number of samples in one C/A code period and M is the number of C/A code periods combined.

The working principle of this type of detector is based on the well-known Gold codes (defined in [18-19]), 'delay and multiply' property [10]. When multiplying a Gold code by a shifted version of the same Gold code, the result of the product is a Gold code itself. This property holds for any Gold code [1],[5],[10],[18] and [16-20]. As stated in [12], there is a subtle difference between the 'delay and multiply' method and the pre-correlation differential receiver/detector. The difference is that the pre-correlation differential receiver works on zero-IF (zero intermediate frequency) signals, whereas the delay

and multiply approach uses the receiver working principle to eliminate both the Doppler frequency drift and the IF.

If the input signal can be expressed in the same way as in equation (8), and if the noise term is ignored, when analyzing the signal labelled as S_A in the diagram, it can be deduced that S_A , can be obtained by multiplying a shifted and conjugated version of the input signal by the input signal. Mathematically this can be expressed in the following manner.

$$S_A(nT_s) = S(nT_s) \cdot S^*(nT_s - \tau) \tag{9}$$

$\tau = JTs$, is the time shift applied to the input signal.

Recalling equation (8), ignoring the noise, carrier phase and power terms, and considering an observation interval in which the navigation data terms do not change, we have:

$$S(nT_s) = C\left(nT_s - \varsigma T_{chip}\right) \cdot e^{jw_d nT_s} \tag{10}$$

Therefore

$$S^*(nT_s - \tau) = C(nT_s - \tau - \varsigma T_{chip}) \cdot e^{-j\, w_d (nT_s - \tau)} \tag{11}$$

Substituting $\tau = JTs$ in (9) (which is the product of expressions (10) and (11)) and evaluating the part of the equation in which complex exponentials are multiplied, we have:

$$e^{jw_d nT_s} \cdot e^{-jw_d (nT_s - \tau)} = e^{jw_d \tau} \tag{12}$$

The resulting product is a constant, because w_d and τ can be considered to be constant when taking small observation intervals (this means the assumption will hold when working with small integration times). This fact is reflected in that it is not necessary to perform a frequency search process to detect the GPS signal, because $e^{jw_d \tau}$ is a constant with no frequency information.

The result of evaluating the code product is expressed mathematically in the following equation:

$$C(nT_s - \varsigma T_{chip}) \cdot C((nT_s - \tau) - \varsigma T_{chip}) = C_{new} \tag{13}$$

These new codes, are Gold codes, according to the Gold code 'delay and multiply' property. The correlation peak is placed in the exact same position as in the original code [10].

The theoretical aspects presented, show that the pre-correlation detector does not need to perform a Doppler space search to detect the presence of the GPS signal. Therefore, the detector can be implemented with no further calculations, as the correlation peak appears in the same exact position.

To quantify how well the pre-correlation differential detector (with a FFT implemented correlation) performs in reducing the computational cost, first the computational cost of the standard non-coherent detector over one period, and using the FFT (Fast Fourier Transform) implementation, is evaluated. The non-coherent detector is used for the comparison as it simple and widely used. The block diagram of the non-coherent receiver implemented using the FFT to calculate the correlation, is as follows:

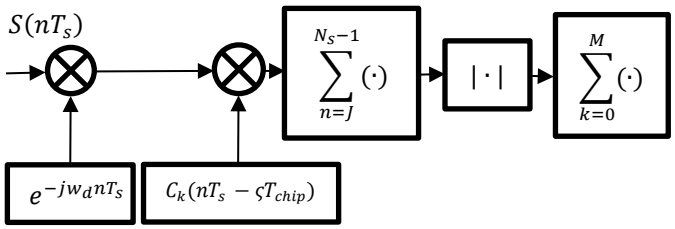

Fig. 2- Non-Coherent detector architecture.

If just 1 ms of signal is processed, and considering a Doppler search span of 100 kHz, using a Doppler frequency step of 100 Hz and being N_s the number of signal samples in 1 ms, then the number of operations is:

$$1000 \cdot (2 \cdot N_s \text{ complex products} + 2 \cdot N_s \text{ sized FFT})$$

The fact (100 kHz/100 Hz) =1000, implies that 1000 frequencies must be explored. This is considered when a factor of 1000 is included in the expression to calculate the number of operations to be performed to process 1 ms of signal.

When examining the block diagram of the pre-correlation differential detector, just two FFT operations and two complex multiplications are performed, therefore the operation count for this detector is:

$$2 \cdot N_s \text{ complex products} + 2 \cdot N_s \text{ sized FFT}$$

At this point, it is important to highlight that one of the shortcomings of this detector is that a Doppler frequency estimation is not obtained. In standard tracking loops, the Doppler frequency must be a known parameter. If no Doppler frequency estimate is available, a tracking loop that implements a differentially coherent tracking loop like the one presented in [21], must be used.

In [6] and [20], the fact no Doppler frequency estimation is obtained is considered an important shortcoming hindering the usage of this type of detector. However, as explained in [22], it is possible to overcome this problem. Using the Parallel Frequency Space Search Acquisition technique, once the correct signal phase offset is obtained, the Doppler frequency can be calculated by multiplying the input signal by a C/A code whose phase has been shifted the same number of phases as the input signal´s phase offset. Once this product is obtained, the FFT of the product

is calculated and a peak in the corresponding Doppler frequency appears, as the spectrum has been unspreaded. After the unspreading process, the original C/A code and carrier signal will only contain the original carrier signal. In case the signal Doppler frequency value is required, then not much additional computational cost is added, because just an additional FFT and an additional complex multiplication are required.

The final computational cost is:

$$3 \cdot N_s \text{ complex products} + 3 \cdot N_s \text{ sized FFT}$$

Since not much computational is added if the Doppler frequency estimation is performed in this fashion, and no more complexity is added in the tracking loop, it is advisable to use the above-mentioned frequency estimation technique.

Theoretical analysis of factors affecting performance

Input Doppler Effect on performance

The feature that motivates the usage of the pre-correlation differential detector is the fact it performs in the same way, no matter the Doppler frequency shift of the input signal. Therefore, it is important to study to which extent and under which assumptions this is true.

According to the mathematical statements included in [5], the expression describing the attenuation, caused by the Doppler frequency of the input signal, and the time delay applied in the type 1 pre-correlation differential operation, is as follows:

$$\alpha_{Doppler}(f_d) = cos\frac{2\cdot\pi\cdot J_c\cdot(f_d/1000)}{L} \quad (14)$$

J_c represents the number of chips the input signal is shifted, *L=1023* (number of chips of the C/A code), $f_{dop}/1000$ is the value of the Doppler frequency of the input signal in kHz. The expression (14) is plotted below, including different values of J_c. From Figure 3, it can be inferred, that the attenuation increases as J_c increases, and that the attenuation increases too as the Doppler frequency increases. As explained in [5], a necessary condition for the pre-correlation differential detector to work is to apply shifts corresponding to an integer number of chips.

In the detector implementation studied in this work, a value of J_c =1 (which corresponds to a value of $J = 2$, if the sampling frequency is twice the chip frequency) is used, as this is the smallest value for J_c.

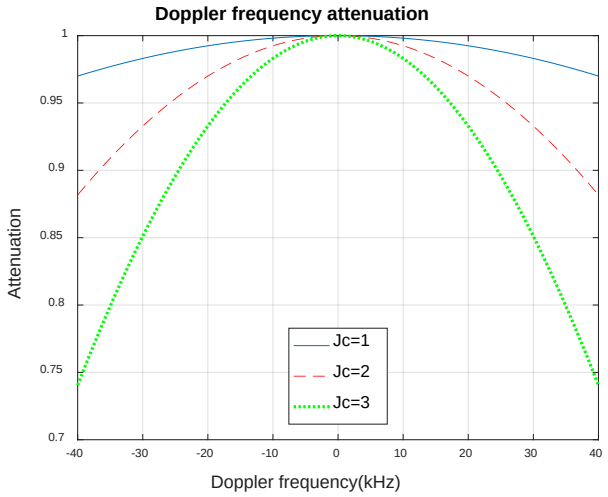

Fig. 3- Pre-correlation differential type 1 detector attenuation for different values for J_c and Doppler frequency.

For $J_c = 1$, the attenuation is negligible for Doppler values below 10 kHz, and an input Doppler bigger than 40 kHz is needed for an attenuation larger than 3 % to happen.

Residual phase error effect on performance

The residual code phase error happens when the estimate for the code phase obtained in the acquisition process does not match the actual code phase. The residual code phase error is the error that affects the receiver performance the most (especially when the sampling frequency is not high) and it does so in a random fashion.

In [5], it is pointed out that as long as the quotient f_d/f_{L1} is close to 0 (in the order of 10^{-5}) the input to the coherent accumulator is the product of two Gold codes. Consequently, the pre-correlation differential receiver behaves in the same way as the coherent detector when considering the residual phase offset. The maximum phase offset error caused by this effect can be quantified recalling the following expression.

$$\theta_{max} = \frac{L}{Ns} \quad (15)$$

Being *L*=1023 (number of chips of the C/A code), and in this work the sampling frequency is 2.041 Msps (Mega samples per second) (this small value is used to minimize the computational cost). When using this sampling value, the quotient L/Ns is approximately 0.5. The actual expression that describes the attenuation caused by this effect is:

$$\alpha_{residual} = 1 - \frac{L}{Ns} \quad (16)$$

If the sampling frequency is 2.041 Msps, the maximum attenuation is close to 50% of the original value. In a LEO scenario, the code Doppler drift is not

negligible. In this scenario, it is advisable to use code compensation.

Data modulation effect

The pre-correlation differential detector/receiver is not affected by the data modulation effect, and a qualitative reasoning can be used to sustain this argument. When analyzing how the signal $S_A(nT_s)$ in Figure 1 is formed, it can be noted that the signal is obtained by multiplying the input signal by a shifted version of the same signal, so when a phase reversal occurs in the input signal, the phase reversal will only affect one sample, as the other samples involved in the product operation will always have the same phase sign. Considering this reasoning, just one sample out of 2041 samples of the resulting product is affected by the data modulation effect and therefore it can be stated that the pre-correlation differential detector/receiver is not affected by the data modulation effect. The same reasoning is included in [5] and [6]. The immunity against the data modulation effect of the detector is demonstrated in the experimental part of this work.

Noise analysis

For the noise analysis, the product $S(nT_s)\cdot S^*(nT_s-\tau)$ must be examined. For simplicity, we ignore the data signal (which can be assumed to be constant for this analysis).

We recall here that $n_w(nT_s)$ follows a Gaussian distribution with power ${\sigma_n}^2$ $(N(0,{\sigma_n}^2))$.
The signals involved are:

$$S(nT_s)=\sqrt{P}\cdot C\left(nT_s-\varsigma T_{chip}\right)\cdot e^{jw_d nT_s}+n_w(nT_s) \quad (17)$$

And:

$$S^*(nT_s-\tau)=\sqrt{P}\cdot C\left(nT_s-\tau-\varsigma T_{chip}\right)\cdot e^{-j\,w_d(nT_s-\tau)}+ {n_w}^*(nT_s-\tau) \quad (18)$$

When multiplying we have:

$$S(nT_s)\cdot S^*(nT_s-\tau)=S_{sig}+S_{n1}+S_{n2}+S_{nn} \quad (19)$$

Where

$$S_{sig}=P\cdot C\left(nT_s-\varsigma T_{chip}\right)\cdot C\left(nT_s-\tau-\varsigma T_{chip}\right)\cdot e^{jw_d\tau} \quad (20)$$

$$S_{n1}=\sqrt{P}\cdot C\left(nT_s-\varsigma T_{chip}\right)\cdot {n_w}^*(nT_s-\tau) \quad (21)$$

$$S_{n2}=\sqrt{P}\cdot C\left(nT_s-\tau-\varsigma T_{chip}\right)\cdot n_w(nT_s) \quad (22)$$

$$S_{nn}=n_w(nT_s)\cdot {n_w}^*(nT_s-\tau) \quad (23)$$

The terms $e^{jw_d nT_s}$ and $e^{-j\,w_d(nT_s-\tau)}$, when multiplied by noise, cause a complex rotation in the noise components, which does not affect their probability density functions [5] and hence will be ignored.
The terms S_{n1} and S_{n2} are zero-mean Gaussian noise terms with power ${\sigma_n}^2$, because if ${n_w}^*(nT_s-\tau)$ or $n_w(nT_s)$ are multiplied by a C/A code, the noise power remains unchanged [23].

At the correlator input the quotient between the signal and noise components is:

$$SN_{prec}=\frac{P\cdot C\left(nT_s-\varsigma T_{chip}\right)\cdot C\left(nT_s-\tau-\varsigma T_{chip}\right)\cdot e^{\mathrm{j}w_d\tau}}{S_{n1}+S_{n2}+S_{nn}} \quad (24)$$

Recalling equation (13) and using the fact $e^{\mathrm{j}w_d\tau}$ is approximately 1 and dividing by $\sqrt{P}$, we have:

$$SN_{prec}=\frac{\sqrt{P}\cdot C_{new}\left(nT_s-\varsigma T_{chip}\right)}{\frac{S_{nn}+S_{n1}+S_{n2}}{\sqrt{P}}} \quad (25)$$

S_{n1} and S_{n2} are the products of shifted noises and C/A codes, and are hence, uncorrelated due to the fact white Gaussian noise is uncorrelated. The noise product term S_{nn} is uncorrelated with the C/A term S_{n1} and S_{n2} contain. Considering S_{n1}, S_{n2} and S_{nn} are uncorrelated processes, the sum of the variances is equal to the variance of the sum of the three processes.

The noise power of the denominator in (25) is

$$E\left[\left(\frac{S_{nn}+S_{n1}+S_{n2}}{\sqrt{P}}\right)^2\right]=\frac{1}{P}\left(E\left[{S_{nn}}^2\right]+E\left[{S_{n1}}^2\right]+E\left[{S_{n2}}^2\right]\right) \quad (26)$$

S_{nn} is the product of two independent Gaussian distributions. According to [24], S_{nn} follows a normal product distribution with variance ${\sigma_n}^4$.

$$E\left[\left(\frac{S_{nn}+S_{n1}+S_{n2}}{\sqrt{P}}\right)^2\right]=2{\sigma_n}^2+\frac{{\sigma_n}^4}{P} \quad (27)$$

Clearly

$$2{\sigma_n}^2+\frac{{\sigma_n}^4}{P}>{\sigma_n}^2 \quad (28)$$

Which means that the signal to noise ratio at the input of the correlator is smaller in the pre-correlation detector than in any detector that does not perform the 'delay and multiply' operation.

For any pre-correlation detector, the noise at the input of the correlator is:

$$2\cdot P\cdot {\sigma_n}^2+{\sigma_n}^4 \quad (29)$$

At the correlator output the noise power is:

$$\sigma_{pre}^2=(M\cdot N_s)\cdot\left(2\cdot P\cdot {\sigma_n}^2+{\sigma_n}^4\right) \quad (30)$$

For the type 1 pre-correlator when forming the decision statistic using the real part, the signal power remains unchanged if $e^{jw_d\tau}$ is close to 1.

However, by taking the real part of the signal, the signal power is divided by two.

$$\sigma_{det}^2 = \left(0.5 \cdot (M \cdot N_s) \cdot \left(2 \cdot P \cdot {\sigma_n}^2 + {\sigma_n}^4\right)\right) \quad (31)$$

The decision statistic is formed by accumulating independent variables, hence by invoking the Central limit, the resulting distribution can be assumed to be Gaussian under both H0 and H1 hypotheses [23].

Under H0 the decision statistic follows a zero-mean Gaussian distribution $N(0, \sigma_{det}^2)$.

Under H1 the decision statistic follows a non-zero mean Gaussian distribution $N(\mu, \sigma_{det}^2)$.

Where

$$\mu = M \cdot N_s \cdot P \quad (32)$$

The probability of false alarm and the detection probability are given by

$$P_{fa} = \frac{1}{2} \cdot erfc\left(\frac{V_{th}}{\sqrt{2 \cdot \sigma_{det}^2}}\right) \quad (33)$$

$$P_d = \frac{1}{2} \cdot erfc\left(\frac{V_{th} - \mu}{\sqrt{2 \cdot \sigma_{det}^2}}\right) \quad (34)$$

Where V_{th} is the decision threshold and erfc is the complementary error function.

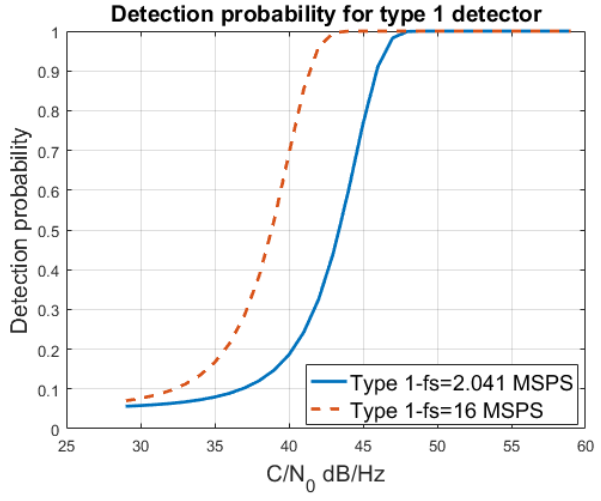

Fig. 4- Detection probability graph for a 10 ms integration time and different sampling frequencies. Pfa=0.02.

Two detection probability for a false alarm probability of 0.02 traces are shown. The continuous traces shows the detection probability for the proposed sampling frequency, whereas the dotted line shows detection probability if a times 8 oversampling scheme is used. Performance increases at the expense of an increased computational cost.

RECEIVER ARCHITECTURE TYPES

The pre-correlation differential detector can be implemented in different manners because it is possible to generate the decision statistic in diverse ways. The decision statistic is formed using just the real part of the correlation result, or generating the statistic using the modulus. A hybrid detector is studied too, as the decision statistic is formed in a differential fashion, by combining correlation results from different C/A periods. These detectors are studied in order to find out if slight implementation changes improve the detector performance.

Type 1 receiver

The type 1 receiver is considered the baseline receiver, upon which, the others are formed by applying slight modifications.

The decision statistic is formed by taking the real part of the correlation result, because the correlation output function describing the attenuation caused by input's signal Doppler frequency depends on the term $e^{j \cdot w_d \cdot T_s \cdot J}$. When the argument of this attenuation function is small, the imaginary part of the term is close to zero, and there is no need to use the imaginary part to form the decision statistic. However, if the Doppler frequency increases some energy moves to the imaginary part.

The decision statistic is found to follow a zero mean Gaussian distribution under the H0 (no signal present) hypothesis and a non-zero mean Gaussian distribution under the H1 (signal present) hypothesis. This is explained by the fact the decision statistic is formed by taking the real part of the correlation.

Type 2 receiver

The type 2 receiver is a modified version of the classical pre-correlation differential receiver. In this case, the decision statistic is formed by taking the modulus of the correlation result.

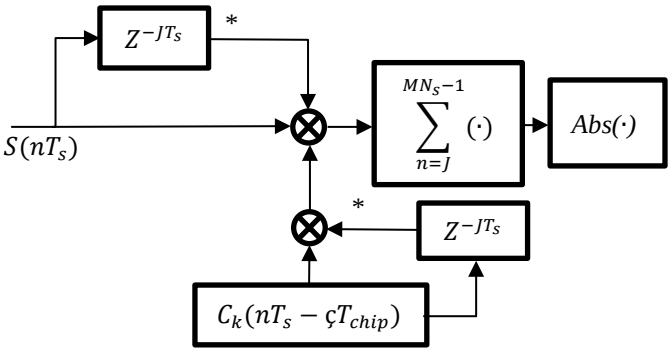

Fig. 5- Type 2 detector

Examining the product $w_d \cdot T_s$, it is important to consider that for an earth based user, w_d takes values of tens of rad/s and T_s takes values of microseconds, then it follows that the product must have a small value. However, in a high dynamic GNSS scenario as the one studied in this work, the values of w_d are 10 times larger than the values of w_d in an earth based receiver and the argument of $e^{j \cdot w_d \cdot Ts \cdot J}$ is 10 times larger. As the value of w_d gets larger, more energy moves to the imaginary part of the exponential and it might be interesting to use the imaginary part to form the decision statistic as proposed in [5].

Therefore, it is interesting to study if in a high dynamic scenario, type 2 receiver, outperforms type 1 detector (bearing in mind the fact in type 1 detector the decision statistic is formed using the real part of the correlation and this reduces the noise power). The distribution of this detector is found to follow a Rayleigh distribution under the H0 hypothesis and a Rice distribution under H1. This fact is consistent with the theoretical argument included in [25]. This argument sustains that a Rayleigh distribution is obtained when the absolute value (magnitude) of a complex number whose components are Gaussian is calculated. When the magnitude operation is applied to non-zero Gaussian variables, the distribution changes from a Rayleigh to a Rice distribution.

Type 3 and 4 receivers

In [12], the Doubly-differential detector is presented. Type 3 and 4 detectors are implemented using this approach. The Doubly-differential detector consists in a pre-correlation differential operation like in type 1 and 2 detectors, followed by a post-correlation multiplication of 1 ms separated correlation outputs. For the type 3 detector, the decision statistic is formed using the real part of the correlation result, whereas for type 4 detector the decision statistic is formed using the modulus of the correlation result. In Figure 6, type 3 and 4 detectors are represented. Type 4 detector is identical to type 3 detector, except in that the decision statistic is formed using the modulus instead of the real part. The output correlations are obtained in the same fashion as for type 1 and 2 detectors, but one of the correlations is delayed $L \cdot T_{chip}$ seconds with respect to the other. The final decision statistic is formed by multiplying two delayed correlation outputs. This detector design pursues a reduction of the noise interfering in the decision statistic. According to [1] and [7], the signal components, should be correlated, whereas the noise components should be independent. Using this procedure, the correlation peak value, should not be affected, and the noise should be reduced. However, in a high-dynamics environment, the fast time-varying Doppler shift might imply the performance is not as good as expected. Furthermore, the post correlation differential product introduces more noise terms in the same way the pre-correlation operation does. Hence, this detector should perform worse. This hypothesis is studied using statistical comparisons of simulation results.

To deduce the decision statistic distributions for type 3 and 4 detectors, the same analysis as for type 1 and 2 detectors is performed. For the type 3 detector, the decision statistic distribution is found to follow a Gaussian distribution, whereas for type 4, the decision statistic follows the same distributions as for type 2.

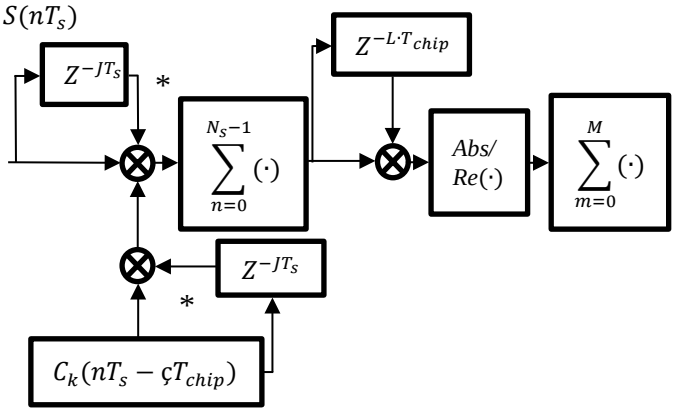

Fig. 6- Type 3 and 4 detectors.

It is interesting to point out, that a detector based on the pre-correlation differential detector is implemented in [6], using the pre-correlation differential detector preceded by a coherent detector. In fact, the author states that this receiver improves performance by improving the receiver sensitivity for low signal level scenarios. Furthermore, in [6], the author aims to design a detector with the pre-correlation differential detector immunity to Doppler, data modulation effects, and the coherent detector sensitivity performance. In the LEO case study, the detector sensitivity is not a problem and thus this approach is not considered in this work.

METHODOLOGY

General aspects

The theoretical aspects presented are validated using a SDR philosophy to implement receiver architectures. A Spirent GSS7700 GNSS signal generator is used to generate the GPS signal for a GPS receiver embedded in a LEO satellite, using the following configuration:

- Full L1 CA constellation in which the Doppler frequency changes.
- The receiver is placed in a 1000 km LEO.
- Variable received signal power.

The experimental setup comprises three major blocks: Spirent GSS7700, USRPX310 and a PC. The simulated GNSS signal is digitized and down-

converted using an USRPX310 device as RF front-end. The samples are fed to a PC, in which MATLAB routines implement the detectors/receivers under test.

The study will start by measuring the performance of the acquisition process for a non-coherent receiver/detector. The results obtained in this baseline case are used to compare the figures of merit of the detectors under study. For the baseline, non-coherent detector, a Doppler frequency search span from [-50 kHz to 50 kHz], with a Doppler frequency search step of 10 Hz is used (this search space is used to minimize the effect of the residual Doppler frequency).

Performance metric

Considering that the pre-correlation detector is a promising technique regarding execution time speed, it is interesting to find out if the detector performance in the LEO GNSS receiver study is acceptable, for different Doppler frequency conditions. In order to measure detector performance, a widely used figure of merit is the deflection coefficient (which is the ratio between the square of the difference of the means under H1 and H0 hypotheses and the variance under H0) as defined in [16] and [26], however according to [26] and [27] this detection metric cannot be used in cases in which receivers with decision statistics with different probability distributions have to be compared, as the comparison by means of the deflection coefficient magnitude can be misleading (as it fails in correctly comparing performance between different acquisition strategies). Another aspect to consider is the deflection coefficient paradox defined in [26] i.e. when using a detector in which the detection statistic is formed via a squaring operation, the deflection coefficient increases without increasing performance. This is another factor advising against the usage of this performance metric. Therefore, the deflection coefficient can only be used to compare the performance of a detector in different scenarios. As stated in [28], the receiver's output SNR cannot be used to fully characterize the receiver detector.

A reliable procedure to measure detector performance is to use the ROC (Receiver Operation Curves) as in [25]. The ROC relates the detection probability, and the false alarm probabilities for a fixed signal strength. However, in the simulated scenario, the input signal power is 47 dB/Hz, so in fact the detection probability in absence of unwanted effects is very close to 1 (for a 10 ms integration time), so there is a need to find a method to measure performance for different Doppler frequency signals. Considering this fact, the ROC curves and ROC based figures of merit such as the equivalent coherent SNR defined in [29] and [30] cannot be used to measure detection performance in this scenario, and some other performance metric must be used.

The new figure of merit is obtained by comparing the maximum value corresponding to the correlation for the null hypothesis H0 (no signal present), with the maximum value of the correlation for the H1 hypothesis (signal present). The maximum value for H0 is obtained by correlating the signal with a local code which is not broadcasted by any satellite. In this way, the margin separating the H0 and H1 hypotheses is measured. The bigger the margin is, the easier it is to distinguish between the two hypotheses. This figure of merit can be defined as a worst-case figure of merit because it does not use the mean value of H0 for the comparison. Instead, it uses the maximum value of H0, establishing a harsher comparison criterion.

Statistical analysis description

The final aim of the statistical analysis, is to detect significant differences in the performance of different detectors and to detect if the performance of a specific detector changes when processing signals with different mean Doppler frequencies or when processing signals that have been modulated by GPS data or signals that have not been modulated.

The data is arranged in 5 different sets formed by 600 GPS signals. Each set is characterized by its own mean Doppler frequency. In order to fully characterize the scenario, it is necessary to repeat the experiment by storing the signal the same number of times as the experiment is repeated, obtaining statistical distributions that can characterize the receiver's behaviour for the case studied. This procedure allows to compare the performance for different Doppler frequencies and to study the effect of data modulation.

The data used is described in a more specific manner now. Each of the 5 sets of 600 signals, can take one of the following mean Doppler frequencies: 0 Hz, -18 kHz and -30 kHz. (Groups 1, 2 and 3 respectively). Groups 1a and 3a correspond to the Doppler frequencies 0 Hz and -30 kHz, but the signals included in the groups 1a and 3a have been modulated by a GPS navigation data signal. By comparing group 1 with group 1a, and group 3 with group 3a the effect of data modulation can be inferred.

The comparison procedure consists in calculating the mean and standard deviation for the figure of merit of each of the 600 signal groups. Using probability density functions and the mean and standard deviation, it is possible to determine if performance changes for different receiver implementations and for different signal conditions. Comparisons between receiver/detector architectures, mean Doppler frequency groups and modulated and unmodulated signals are carried out.

The figure of merit obtained after processing each signal forming part of particular Doppler set is arranged to obtain the probability density functions, which characterize the performance of a specific Doppler group. For each type of detector under test, the Doppler frequency groups are compared. In this way, the detector behaviour under different Doppler

scenarios is characterized.

Using a fixed Doppler frequency, the distributions formed by the figures of merit for each method are compared. In this way, the performance of the detector under test can be studied.

The other important aspect to be studied is the execution time for each receiver. The execution time for the different acquisition algorithms is measured and compared. The differences are studied to validate the theoretical statement that asserts that the pre-correlation differential detector execution time is remarkably smaller than the execution time for baseline non-coherent algorithm.

RESULTS

Non-Coherent detector (unmodulated signal)

First, the performance results for the 3 Doppler frequency groups for the non-coherent detector, are presented for the dataset of signals that are not data modulated. A 10 ms integration time is used. The figure of merit for all the signals contained in each of the 3 Doppler frequency groups is calculated. The mean and the standard deviation of each of the 3 Doppler groups are presented, and the probability distribution functions for the three groups are examined. In Table 1, the values for the mean and standard deviation of the 3 groups are shown, using the non-coherent detector with a frequency search step of 10 Hz. The receiver code replica chip frequency has been adjusted taking into account the code Doppler effect.

The probability distributions for the three Doppler frequency groups are obtained and shown in Figure 7.

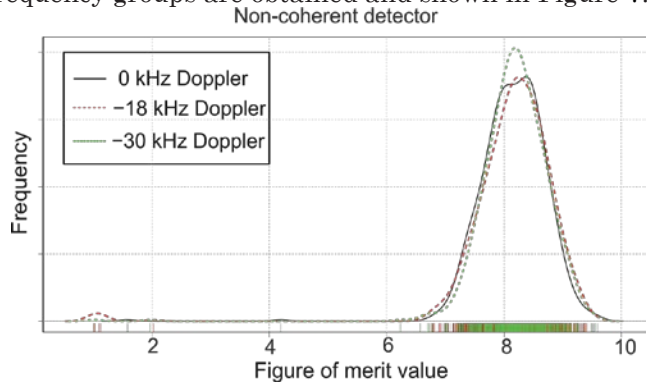

Fig. 7- Decision statistic distribution for the figure of merit of the three Doppler frequency groups for the non-coherent detector.

When analyzing Figure 7, it important to highlight that the signals do not contain GPS data, and that the attenuation caused by the Doppler frequency residual error is negligible as the Doppler frequency search bin used in this case is 10 Hz, and a 10 Hz residual Doppler results in a negligible attenuation [1] and [5-6]. Hence, the only effect (if the noise level is kept constant) that can affect the signal's figure of merit is the residual code offset error. The variability is large, and this is explained by the fact the sampling frequency is close to twice the code chip frequency. In fact, as stated in equation (16), when the sampling frequency is twice the chip frequency, an attenuation of 50 % of the theoretical value can be obtained. As expected, the figure of merit shows that performance is similar for the three Doppler frequency groups.

The execution speed is assessed by measuring the non-coherent acquisition execution time, 1000 times for each of the 600 signals integrating a Doppler group. The mean execution time is used as the estimator of the execution time. A 100 Hz frequency search step is used in this case (instead of the 10 Hz frequency search step used to obtain the figure of merit), and the Doppler search space spans from [-50 kHz to 50 kHz]. A 100 Hz frequency search step has been used instead of a 10 Hz, because this search step value yields the same frequency resolution than the proposed procedure to obtain the Doppler frequency for the pre-correlation detector. The experiment is performed and the mean execution time for the non-coherent detector is found to be 80.165 s.

Table 1- Figure of merit mean and standard deviation for Doppler frequency groups for the non-coherent detector.

Doppler	0 kHz	-18 kHz	-30 kHz
Mean figure of merit	8.15	8.12	8.18
Standard Deviation	0.58	0.91	0.62

Pre-correlation differential detector (non-modulated signal)

Figure of merit results

In Table 2, the mean and the standard deviation of the figures of merit resulting of the signal processing, using pre-correlation differential detectors are presented. For the experiment, a 10 ms non-coherent integration time is used. In table 3 the normalized deflection coefficient for type 1 detector is presented to highlight the great degree of correlation between the designed figure of merit and the deflection coefficient in measuring performance in different Doppler scenarios.

In order to estimate the execution time, the acquisition algorithms are executed 1000 times for each of the 600 signals and the mean execution time measured using timing routines is used as an estimate. The same signals as the ones used to measure the execution time of the baseline non-coherent detector, are processed using the pre-correlation differential detector. The correlations for the pre-correlation differential detector have been implemented using the FFT method. Therefore, the procedure used to measure the execution time was exactly the same for the two

algorithms. The mean acquisition execution time is 0.092 s instead of the 80.165 s needed using the baseline method.

Table 2- Figures of merit mean and standard deviation for different Doppler frequency groups and different pre-correlation differential detectors.

Doppler/Type		0 Hz.	-18 kHz.	-30 kHz.
Type 1	Mean	5.75	5.60	5.78
	S.D	0.66	0.73	0.66
Type 2	Mean	3.83	3.94	4.00
	S.D	0.28	0.39	0.31
Type 3	Mean	2.48	2.49	2.52
	S.D	0.37	0.38	0.40
Type 4	Mean	2.22	2.23	2.24
	S.D	0.32	0.31	0.33

Table 3- Deflection coefficient for type 1 detector

Deflection coefficient		0 Hz.	-18 kHz.	-30 kHz.
Type 1	Mean	2.46	2.38	2.40

In Figure 8, the correlation results obtained by processing the same signal with different detectors are presented. It is shown that the acquisition peak appears with the same phase offset, for the two

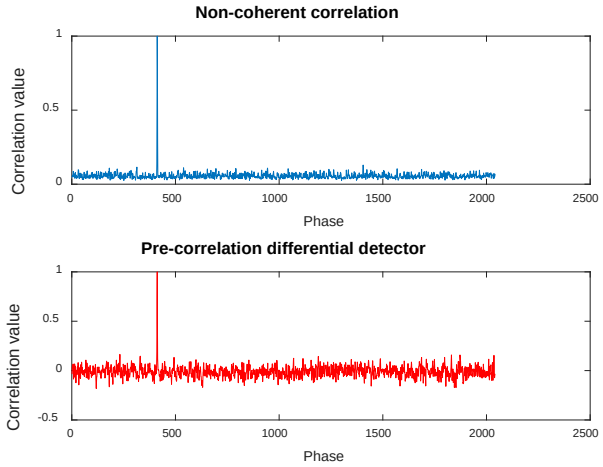

Fig. 9- Correlation peak for different receiver architectures.

detector architectures compared. This behavior matches the theoretical statement asserting that the code phase obtained with the two detectors must match. For the pre-correlation differential detector, the difference between the correlation peak value and the correlation noise is smaller than for the non-coherent detector.

Doppler frequency estimation

The concepts presented in [19] can be used to obtain an estimate for the GPS signal Doppler frequency. First, the input GPS signal is multiplied by a shifted version of the C/A code (the number of shifted samples must correspond to the phase offset obtained using the pre-correlation differential detector).

Once the input signal is multiplied by the shifted C/A code, the GPS signal is de-spreaded. If the FFT of the de-spreaded signal is calculated and plotted, a peak corresponding to the Doppler frequency appears. The process is applied to a 10 ms signal, hence the frequency resolution of the FFT is 100 Hz, [31]. In Figure 9, the top graph, shows the entire frequency spectrum, and the in the bottom graph, a zoom in operation near the peak area is applied to determine

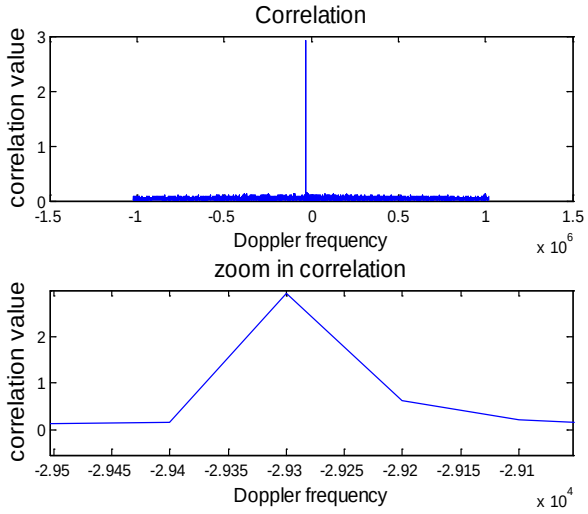

Fig. 8- Doppler frequency estimation using the phase estimate.

the Doppler frequency value.

The Doppler frequency is found to be -29.4 kHz, instead of 29.3 kHz, which is the actual Doppler frequency. The estimation error is equal to the FFT frequency resolution; therefore, the Doppler frequency estimation is successful.

Input Doppler Frequency effect Analysis

The statistical analysis intends to find out if statistically significant differences between the figures of merit of the signals that form each Doppler frequency group can be detected. In fact, this is the same statistical analysis procedure as the one used for the non-coherent detector. For each frequency group, the figures of merit of each signal are processed to obtain the probability density function. This analysis is useful to determine if significant differences in the characteristic probability density plots exist. Moreover, if differences are detected, the procedure helps in determining between which frequency groups

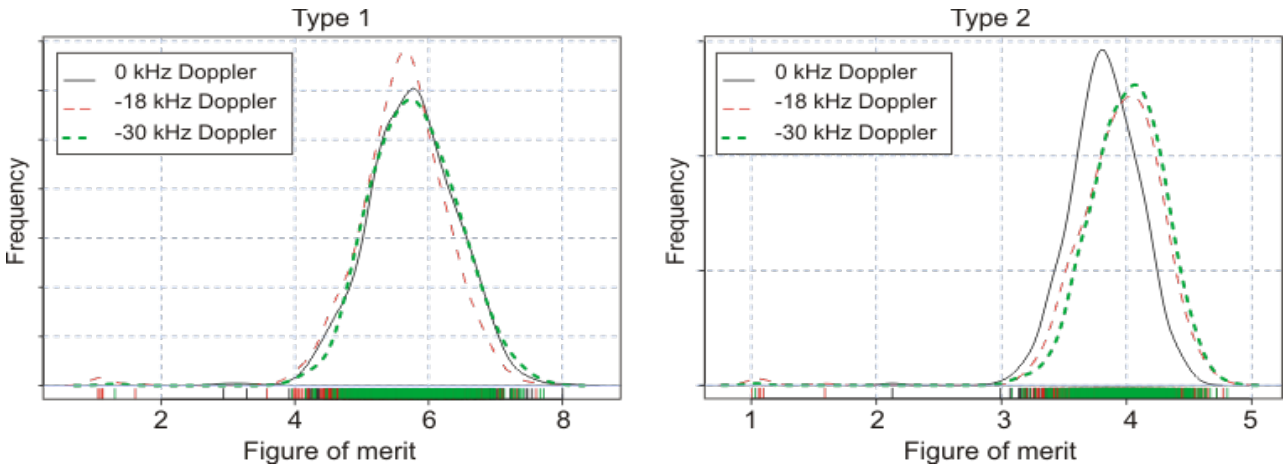

Fig. 10- Probability density plots for the figures of merit of type 1 and 2 detectors.

these differences appear. As stated, each of the three groups is composed by a set of 600 signals which are not modulated by navigation data and are sharing the same Doppler frequency. The first case study deals with the study of the effect of the Doppler frequency on the classical pre-correlation differential detector. The objective is to demonstrate that the receiver works well despite the signal's Doppler frequency.

In Figure 10, the frequency distributions for type 1 and type 2 detectors are shown. When analyzing the frequency distributions, it is important to point out that the characteristic group probability density functions overlap in the vast majority of points. This fact sustains the idea the performance is similar for the three frequency groups. Therefore, in a practical, real world application, it can be concluded that the pre-correlation differential detector is coping well with high input Doppler frequency GPS signals. The results demonstrate that the receiver performance is virtually invariant to the input frequency. Hence, this detector can be used in high dynamic applications as the performance is not affected by the frequency, and the execution time speed-up is large. It is true, however, that for type 2, the 0 kHz group performs slightly worse. The major drawback of the method is that the figure of merit is approximately 6, whereas for the non-coherent detector the figure of merit is near to 8. This means that for this case a bigger difference between the H0 hypothesis maximum value and the H1 hypothesis maximum value is obtained if the baseline non-coherent receiver is used. Therefore, the baseline detector performs better, but the difference in performance is not very large.

The probability density distribution comparison for type 3 and type 4 detectors, shown in Figure 11 reveals that, in fact, the probability distributions for the 3 groups with different mean Doppler frequency are similar. Therefore, the detector is working well despite the signal's input Doppler frequency.

Using an experimental setup, it has been demonstrated that all the pre-correlation differential forms presented are immune to the Doppler effect.

Receiver architecture performance comparison

Once the receiver's Doppler behaviour has been characterized, the next step is to obtain a receiver/detector architecture comparison i.e. comparing detector performance for different detector architectures.

To do so, the figures of merit of 600 signals belonging to the same Doppler frequency group are calculated, and a statistical study to compare receiver performance is carried out.

According to figure 10, detector types 1 and 2, are detectors that do not build the decision statistic using

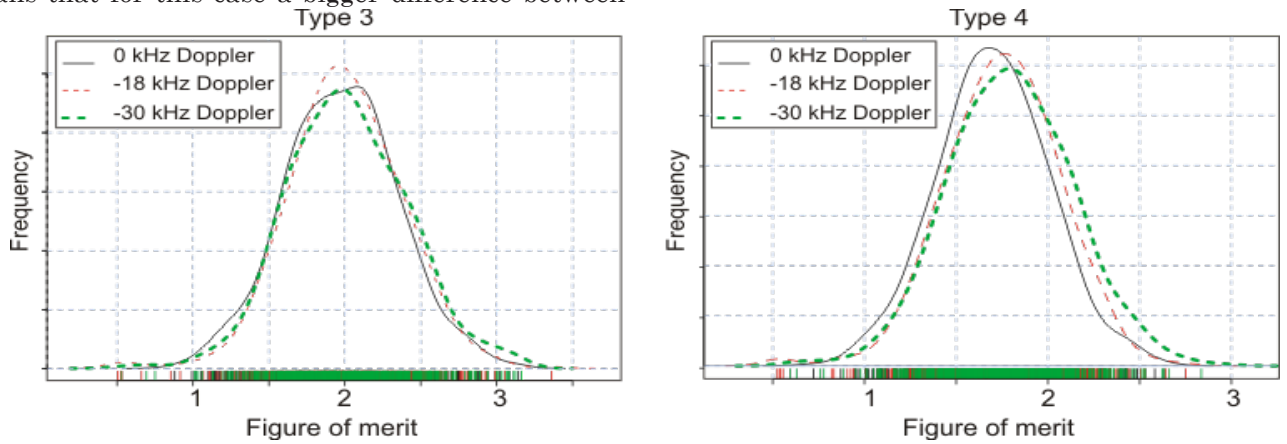

Fig. 11- Probability density plots for figures of merit for types for type 3 and 4 detectors.

differential products. These detectors perform much better than detector types 3 and 4, which build the decision statistic using a differential product.

The receiver/detectors that generate the decision statistic using the real part of the correlation result (type 1 and 3 detectors) perform better than receivers in which the decision statistic is formed using the modulus of the correlation result, no matter the input signal Doppler frequency.

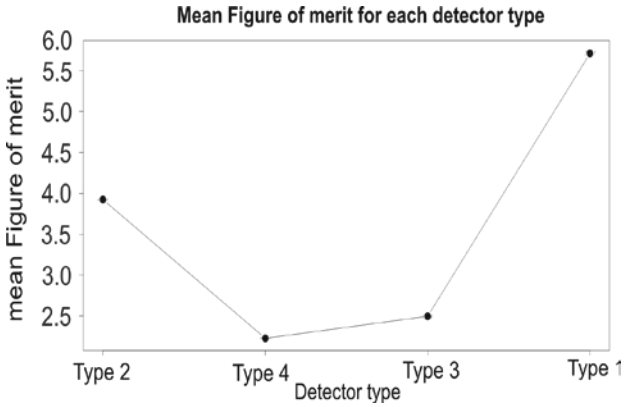

Fig. 12- Detector figure of merit means.

From Figure 12 it can be concluded, that for the case study, the detector to be used should be based on type 1 detector, as it outperforms the other detector types.

Data modulation effect analysis.

To analyze the data modulation effect on receiver performance, comparisons using signals with the same Doppler frequency are performed. Two sets of 600 signals are compared in Figure 13. The two sets are characterized by a mean input Doppler frequency of 0 kHz (group 1 is compared with group 1a), and one set contains data modulated signals, whereas the other contains unmodulated signals. The figure of merit for the signals is calculated, and the results are arranged into two probability frequency distribution graphs. The graph shows that the two signal sets behave similarly. The same study is performed to compare group 3 with group 3a) and, again, the two signal sets behave similarly.

The frequency distributions shown in the two graphs agree with the theory, as they point out that the data modulation has virtually no effect on the receiver performance.

DISCUSSION.

The evidence presented backs up the idea that the receiver/detector is working as expected, because despite slight performance differences are observed between Doppler frequency groups, these differences have no correlation with the group mean Doppler frequency value. Therefore, the observed differences are caused by the non-ideal behaviour of elements in the experimental setup and signal residual effects. The statistical frequency distribution analysis shows that the Doppler frequency group behaviour is similar, and that in a realistic simulation no behaviour differences caused by the Doppler frequency are appreciated. This argument is sustained by the fact that the values for the figure of merit of the 0 kHz Doppler frequency group have not been greater than for the other group values, so the detector is not performing better for low Doppler frequencies. The demonstrated invulnerability to high input Doppler frequency values, which is presented in the theoretical analysis and validated experimentally, suggests that the receiver is suitable for the case study.

An aspect to be highlighted is the fact that, if the probability density functions for detector architectures (as the one shown in Figure 7) are analyzed, the residual phase offset effect makes the figure of merit change substantially and in random fashion. This is explained by the small sampling frequency used to reduce the computational cost. As stated in the theoretical discussion this effect affects both the baseline non-coherent detector and the pre-correlation differential detector to the same extent. The performance comparison between the baseline non-coherent and the different pre-correlation differential detectors points out that the non-coherent detector performs better.

The figure of merit comparison for groups containing navigation data and groups that do not, shows that the receiver is not affected by the presence of the data

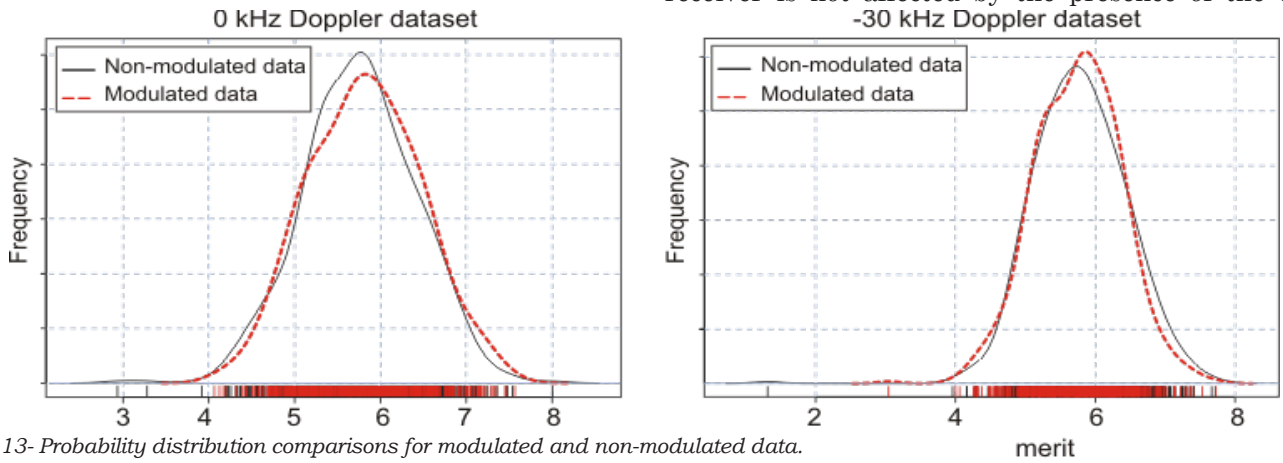

Fig. 13- Probability distribution comparisons for modulated and non-modulated data.

signal, i.e. it is immune to the presence of this signal. This fact is stated in the theoretical analysis, and confirmed by the results presented in Figure 13

Statistical distributions for each receiver/detector are obtained. For detectors that generate the decision statistic using the real part of the correlation result (Type 1 and 3 detectors), the decision statistic is found to be distributed approximately following a Gaussian distribution both for the H0 and H1 hypotheses. On the other hand, detectors that generate the decision statistic using the modulus of the correlation (Type 2 and 4 detectors), result in Rayleigh distributions, for the H0 hypothesis and Rice distributions for the H1 hypothesis. In [7] the H0 hypothesis for type 3 receiver is said to follow a Laplace distribution for low signal power levels, but are said to follow a Gaussian distribution when considering a high signal level case-study so the obtained results match the results presented in [7].

In [5], it is suggested that for scenarios where the input Doppler frequency is high, it might be interesting to generate the decision statistic using the modulus of the correlation result, however the evidence presented here proves that, for the case study, the modulus decision statistic does not improve performance. Nevertheless, it must be stated that in [5], the suggestion is made considering a signal model with no additive noise. An explanation for this can be found if the probability density functions are considered. In Rayleigh distributions, more samples tend to concentrate on the right distribution tail, hence if the maximum value for the H1 hypothesis does not change, the difference between the H0 and H1 hypotheses maximum values decreases. This is the reason behind the decreased performance of the decision statistics generated using the modulus. When dealing with type 3 and 4 detectors, the decision statistic is generated using the differential product. From the experiments performed, it is confirmed that the correlation peak decreases, so the figure of merit does not improve. So, in fact, in a high dynamic context, the two differential inputs are not as correlated accounting for the fast frequency variations caused by the dynamic stress. Therefore it is confirmed that the doubly differential architecture does not work well in this scenario.

Beyond detection, the other key aspect is the execution time. The pre-correlation differential detector improves the acquisition time by a factor of 1000, at the expense of a slightly decreased signal quality. Recalling the above-mentioned aspects, it can be stated that pre-correlation differential implementation using the real part decision statistic is feasible for a high dynamic scenario, because of the 1000 times speed-up. In addition, the worsening of the detector performance in comparison with the non-coherent detector is not so important when considering that for a LEO satellite the signal level is high and that each time GNSS systems are updated, the transmitted power increases substantially.

The Doppler frequency estimation procedure works perfectly and it is proved that the estimation procedure is not computationally burdensome. This result agrees with the theoretical computational cost study performed. Therefore, the procedure can be employed, and the pre-correlation differential detector can be used along with a standard tracking loop.

CONCLUSIONS

A SDR experimental setup is used to implement a technological demonstrator for detector/receiver architectures in a realistic LEO scenario. The pre-correlation differential detector for the LEO context has been studied theoretically to evaluate its suitability for the case study. Moreover, the receiver's suitability for the case study (especially bearing in mind GNSS evolutions with increased power) has been validated experimentally using a Spirent GSS7700 signal generator to generate a realistic scenario. The detector has been able to acquire signals without performing a frequency search.

An ad hoc figure of merit has been designed and used to evaluate the detector performance. The figure of merit has been used to show that the pre-correlation differential detector can be used in this high signal level scenario.

The residual effects affecting the pre-correlation differential detector performance, such as the data modulation and the residual phase offset effect, have been studied. Using the standard pre-correlation differential detector presented as the starting point, different modified architectures have been implemented and evaluated in a LEO scenario. The architecture that generates the decision statistic using the real part of the correlation result performs the best. Each detector variety has been characterized by means of statistical distributions, which help in describing the detector performance. The figure of merit decreased performance in the pre-correlation differential detector in comparison to the non-coherent detector has been quantified. This information is useful in future applications, as it can be used as a reference.

The speed-up has been quantified by comparing the execution time of the non-coherent detector and detectors under test. The large speed-up obtained suggests that for the case of a LEO satellite in which constraints linked to the receiver movement, imply a fast acquisition is needed, the proposed detector is a suitable choice. Furthermore, LEO satellites, generally have limited power capabilities, and a method as the one proposed in the paper can help in energy management issues. A method to estimate the Doppler frequency is successfully used, and it is demonstrated that this method does not increase the computational cost substantially.

Recalling the large speed-up and signal quality reported, it has been demonstrated theoretically and empirically that a GPS receiver based on this receiver/detector architecture is feasible in a LEO scenario.

REFERENCES

1. Calmettes, V., Dion, A., Boutillion, E. and Liegeon, E., "Fast Acquisition Unit for GPS/GALILEO Receivers in Space Environment", *Proceedings of the 2008 National Technical Meeting of The Institute of Navigation,* San Diego, CA , 2008 pp. 288 - 297
2. Hauschild, A., Markgraf, M. and Montenbruck, O., "GPS receiver performance on board a LEO satellite*", Inside GNSS,* 2014, pp 48-57.
3. Esteves, P., "Techniques d'acquisition à haute sensibilité des signaux GNSS", PhD Thesis, *Institut Supérieur de l'Aéronautique et de l'Espace (ISAE)*, 2014.
4. Zolesi, B. and Cander, L. R., "Ionospheric Prediction and Forecasting", *Springer Geophysics, Springer-Verlag*, 2014.
5. O' Driscoll, C., "Performance Analysis of the Parallel Acquisition of Weak GPS Signals", *University College Cork*, 2007.
6. Shanmugam, S.K., "New Enhanced Sensitivity Detection Techniques for GPS L1C/A and Modernized Signal Acquisition", PhD Thesis, *University of Calgary*, Calgary, Alberta, 2008.
7. Esteves, P. and Boucheret, M., "Sensitivity characterization of differential detectors for acquisition of weak signals*", IEEE transactions on aeorospace and electronic systems*, Vol. 12, No. 1, 2016, pp 20 – 37.
8. Foucras, M., "Performance analysis of modernized GNSS signals GNSS", PhD Thesis, *Institut Supérieur de l'Aéronautique et de l'Espace (ISAE)*, 2015.
9. Akopian, D., "Fast FFT based GPS satellite acquisition methods", *IEE Proceedings on Radar, Sonar & Navigation*, Vol. 152, No. 4, 2005, pp 277-286.
10. Bao-Yen Tsui, J., "Fundamentals of Global Positioning System Receivers. A Software Approach", *John Wiley & Sons, Inc.*, New York, 2000.
11. Winternitz, L.M.B., Bamford W.A. and Heckler,G., "A GPS receiver for High-altitude satellite navigation", *IEEE Journal of selected topics in signal processing*, 2009,pp 541-556.
12. Shanmugam, S.K., Watson R., Nielsen, J., and G Lachapelle "Differential Signal Processing *Schemes for Enhanced GPS Acquisition", Proceedings of the 18th International Technical Meeting of the Satellite Division of The Institute of Navigation (ION GNSS 2005),* Long Beach, 2005, pp. 212 – 222.
13. Birklykke, A., "High Dynamic GPS Signal Acquistion", Master thesis, *Department of Electronic Systems, Aalborg University*, 2010.
14. Kaplan, E.D., "Understanding GPS: Principles and Applications", *Artech House Publishers*, 1996.
15. Al Bitar, H., "Advanced GPS signal processing techniques for LBS services", PhD thesis, *Institut National polythechnique de Toulouse*, 2007.
16. Shanmugam. S.K "Improving GPS L1 C/A Code correlation properties using a novel multi-correlator differential detector technique", *Proceedings of the 19th International Technical Meeting of the Satellite Division of The Institute of Navigation (ION GNSS 2006),* Fort Worth*,* 2006, pp 2453 – 2464.
17. Hui, Hu. , Yuan, Yuan., Huan Wang. and Minghua Gao., "GPS Receiver C/A Code Rapid Acquisition Technology", *Research Dan Zou School of Information Engineering, East China Jiaotong University*, 2013, pp 477-484.
18. Sarwate, D. V. and Pursley, M. B., "Crosscorrelation Properties of Pseudorandom and Related Sequences", *Proc. of IEEE*, Vol. 68, No. 12, 1980, pp 593-619.
19. Gold R, "Optimal binary sequences for spread spectrum multiplexing", *IEEE Transactions on Information Theory,* Vol. 13, No. 4, 1967, pp 619-621.
20. Arribas Lázaro, J., "GNSS Array-based Acquisition: Theory and Implementation", Ph.D. Dissertation *Centre Tecnològic de Telecomunicacions de Catalunya (CTTC)*, 2012.
21. Fan, C. C. and Tsai. Z. "A differentially coherent delay-locked loop for spread-spectrum tracking receivers", *IEEE Communications Letters*, 1999, pp 282-284.
22. Borre K., Akos D.M. et al, "A Software-Defined GPS and Galileo Receiver: A Single-Frequency Approach", *Ed Birkhauser*, 2007.
23. Zhongliang, D., Yue, X., Jichao, J. and Lu, Y. "Unambigous Acquisition for Galileo E1 OS signal Based on Delay and Multiply" *TELKOMNIKA,* Vol. 12, No. 4, 2014,pp 950-962.
24. Craig, C. C. (1936). "On the Frequency Function of xy", *Annals of Mathematical Society* 1936, pp 1–15.
25. Hippenstiel, R. D., "Detection theory: applications and digital signal processing", CRC Press LLC, 2002.
26. Borio, D., Gernot C., Macchi, F. and Lachapelle, G. "The output SNR and its role in quantifying GNSS signal performance". *Proceedings of ENC, Toulouse, France* ,2008.
27. Macchi, F., "Development and Testing of an L1 Combined GPS-Galileo Software Receiver", PhD thesis *University of Calgary*, 2010.
28. Turunen, S., "Weak Signal Acquisition in Satellite Positioning", PhD thesis *Tampere University of Technology*, 2010.
29. Borio, D., "A statistical theory for GNSS signal acquisition", Ph.D.dissertation*, Politecnico de Torino*, 2008.
30. Borio, D. and Akos, D. "Noncoherent Integrations for GNSS Detection: Analysis and Comparisons", *IEEE transactions on aeorospace and electronic systems,* Vol. 45, No. 1, 2009,pp 360-375*.*
31. Proakis, J.G. and Manolakis, D. G, "Digital Signal Processing. Principles, Algorithms, and Applications", *Prentice Hall*, 1996.